Article

Toward Binary Nitrosyls: Distinctly Bent Fe–N–O Linkages in Base-Stabilized Fe(NO) Complexes

Trevor W. Hayton, W. Stephen McNeil, Brian O. Patrick, and Peter Legzdins

J. Am. Chem. Soc., **2003**, 125 (42), 12935-12944• DOI: 10.1021/ja036887r • Publication Date (Web): 27 September 2003

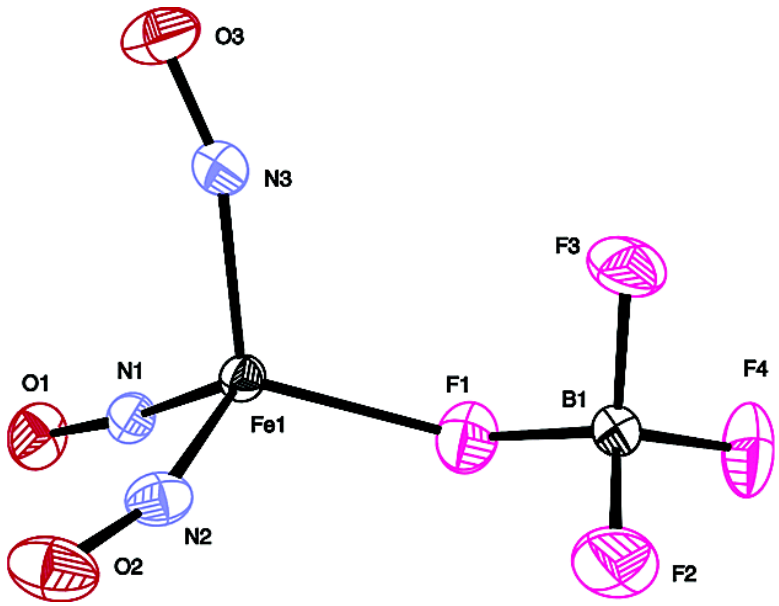

More About This Article

Additional resources and features associated with this article are available within the HTML version:

- Supporting Information
- Access to high resolution figures
- Links to articles and content related to this article
- Copyright permission to reproduce figures and/or text from this article

View the Full Text HTML

J|A|C|S
ARTICLES
Published on Web 09/27/2003

Toward Binary Nitrosyls: Distinctly Bent Fe−N−O Linkages in Base-Stabilized $Fe(NO)_3^+$ Complexes

Trevor W. Hayton,[†] W. Stephen McNeil,[‡] Brian O. Patrick,[†] and Peter Legzdins*,[†]

Contribution from the Department of Chemistry, University of British Columbia, Vancouver, British Columbia, Canada V6T 1Z1, and the Department of Chemistry, Okanagan University College, Kelowna, British Columbia, Canada V1V 1V7

Received June 24, 2003; E-mail: legzdins@chem.ubc.ca

Abstract: Air- and moisture-sensitive $Fe(NO)_3(\eta^1\text{-}PF_6)$ (**1**) may be conveniently prepared by treating $Fe(NO)_3Cl$ with 1 equiv of $[Ag][PF_6]$ in CH_2Cl_2 or by reacting $[NO][PF_6]$ with excess iron filings in $MeNO_2$. Complex **1** is thermally sensitive both as a solid and in solutions, and is best handled below −20 °C. To isolate **1** reproducibly from $MeNO_2$ solutions it is necessary to remove all traces of propionitrile, which often occurs as an impurity in $MeNO_2$, because it reacts with Lewis-acidic **1** to form $[Fe(NO)_3(EtCN)][PF_6]$ (**2**). If trace H_2O is present during the synthesis of **1**, some of the PF_6^- is converted to $PO_2F_2^-$, which is sufficiently Lewis basic that it captures two $Fe(NO)_3^+$ fragments and forms $[(ON)_3Fe(\mu\text{-}PO_2F_2)Fe(NO)_3][PF_6]$ (**3**). Finally, $Fe(NO)_3(\eta^1\text{-}BF_4)$ (**4**) can be obtained as a green microcrystalline powder by employing the same synthetic methodologies used to prepare **1**. The new complexes **1**−**4** have been characterized by conventional spectroscopic methods, and the solid-state molecular structures of **2**, **3**, and **4** and their parent compound, $Fe(NO)_3Cl$, have been established by X-ray diffraction methods. The iron centers in the $Fe(NO)_3$ fragments in all these structures exhibit approximately tetrahedral coordination geometries, and the Fe−N−O linkages are distinctly nonlinear with bond angles in the range of 159 to 169°. DFT calculations on $Fe(NO)_3(\eta^1\text{-}BF_4)$ (**4**) confirm that its bent Fe−N−O links have an electronic origin and need not be attributed to other factors, such as packing forces in the crystal. Interestingly, the bending of the NO ligands results in an increase in the energy of the HOMO, relative to the linear case, but at the same time causes a decrease in energy of the HOMO-1 and the HOMO-2 molecular orbitals. This more than compensates for the higher energy of the HOMO, resulting in a lower energy structure.

Introduction

Homoleptic metal−carbonyl complexes are ubiquitous in modern inorganic chemistry. Not only have they been useful during the development of our fundamental understanding of metal−ligand bonding, they have also found numerous important chemical applications.[1] In contrast, despite the similarities between CO and NO as strong π-acceptor ligands, similar homoleptic metal−nitrosyl complexes are quite rare and poorly studied.[2,3] Only four examples of binary nitrosyls have been reported to date, namely $Cr(NO)_4$,[4−10] $Fe(NO)_4$,[11,12] $Co(NO)_3$,[13] and $[Fe_2(NO)_6]^{2+}$.[14] These complexes have proven to be difficult to study, e.g. $Cr(NO)_4$ has a tendency to spontaneously lose NO, and none has been characterized by single-crystal X-ray crystallography. Among the four reported homoleptic nitrosyl species, $Cr(NO)_4$ is the only one whose formulation and molecular structure are assured, since it has been the subject of numerous infrared and electron-diffraction studies.[6,15] On the other hand, $Fe(NO)_4$, $Co(NO)_3$, and $[Fe_2(NO)_6]^{2+}$ have only been described briefly in the literature, and so some doubt remains as to their true natures. In an attempt to resolve the uncertainty associated with these compounds, we have decided to reinvestigate them, and we began by revisiting $[Fe_2(NO)_6][PF_6]_2$.

The putative $[Fe_2(NO)_6]^{2+}$ species was originally synthesized by a number of methods, including reaction of $Fe(CO)_2(NO)_2$ with $[NO][PF_6]$, chloride abstraction from $Fe(NO)_3Cl$ by $[Ag][PF_6]$, and treatment of iron filings with $[NO][PF_6]$ in nitromethane. It was formulated by Herberhold and co-workers

[†] University of British Columbia.
[‡] Okanagan University College.

(1) Cotton, F. A.; Wilkinson, G.; Murillo, C. A.; Bochmann, M. *Advanced Inorganic Chemistry*; Sixth ed.; John Wiley & Sons: New York, 1999.
(2) Hayton, T. W.; Legzdins, P.; Sharp, W. B. *Chem. Rev.* **2002**, *102*, 935−992.
(3) Richter-Addo, G. B.; Legzdins, P. *Metal Nitrosyls*; Oxford University Press: New York, 1992.
(4) Herberhold, M.; Razavi, A. *Angew. Chem., Int. Ed. Engl.* **1972**, *11*, 1092−1094.
(5) Satija, S. K.; Swanson, B. I.; Crichton, O.; Rest, A. J. *Inorg. Chem.* **1978**, *17*, 1737−1741.
(6) Hedberg, L.; Hedberg, K.; Satija, S. K.; Swanson, B. I. *Inorg. Chem.* **1985**, *24*, 2766−2771.
(7) Guest, M. F.; Hillier, I. H.; Vincent, M.; Rosi, M. *J. Chem. Soc., Chem. Commun.* **1986**, 438−439.
(8) Swanson, B. I.; Satija, S. K. *J. Chem. Soc., Chem. Commun.* **1973**, 40−41.
(9) Chen, H. W.; Jolly, W. L. *Inorg. Chem.* **1979**, *18*, 2548−2551.
(10) Bauschlicher, C. W., Jr.; Siegbahn, P. E. M. *J. Chem. Phys.* **1986**, *85*, 2802−2807.
(11) Griffith, W. P.; Lewis, J.; Wilkinson, G. *J. Chem. Soc.* **1958**, 3993−3998.
(12) Doeff, M. M.; Pearson, R. G.; Barrett, P. H. *Inorg. Chim. Acta* **1986**, *117*, 151−155.
(13) Sabherwal, I. H.; Burg, A. B. *J. Chem. Soc., Chem. Commun.* **1970**, 1001.
(14) Herberhold, M.; Klein, R. *Angew. Chem., Int. Ed. Engl.* **1978**, *17*, 454−455.
(15) Wang, X.; Zhou, M.; Andrews, L. *J. Phys. Chem. A* **2000**, *104*, 7964−7973.

Table 1. Nitrosyl Absorptions in the Solution IR Spectra of $Fe(NO)_3Cl$ and Complexes **1**−**4**

	solvent	
	$MeNO_2$, ν(NO) cm^{-1}	CH_2Cl_2, ν(NO) cm^{-1}
$Fe(NO)_3Cl$	1905 (w), 1795 (s)	1898 (w), 1789 (s)
$Fe(NO)_3(\eta^1\text{-}PF_6)$ (**1**)	1934 (w), 1822 (s)	1922 (w), 1810 (s)
$[Fe(NO)_3(EtCN)][PF_6]$ (**2**)	1942 (w), 1831 (s)	1939 (w), 1836 (s)
$[(ON)_3Fe(\mu\text{-}PO_2F_2)Fe(NO)_3][PF_6]$ (**3**)	1932 (w), 1822 (s)	1923 (w), 1813 (s)
$Fe(NO)_3(\eta^1\text{-}BF_4)$ (**4**)	1934 (w), 1817 (s)	1922 (w), 1814 (s)

as consisting of two $Fe(NO)_3^+$ units linked by an unsupported Fe═Fe double bond, i.e.,

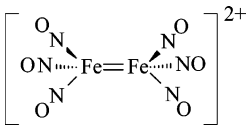

The evidence cited to support such a structure was provided by IR spectroscopy, which demonstrated that no bridging nitrosyls were present in the complex, and conductivity measurements, which suggested that the iron complex was a 1:2 electrolyte.

This contribution describes our reinvestigation of this system in an attempt to establish the structure of the binary iron nitrosyl cation. As a result of our studies, we can now report that the species isolated in 1978 is a monometallic complex, best formulated as $Fe(NO)_3(\eta^1\text{-}PF_6)$. During these investigations, we have also isolated several Lewis-base adducts of the acidic $Fe(NO)_3^+$ species and have discovered that they all exhibit distinctly bent Fe−N−O linkages.

Results and Discussion

Synthesis and Characterization of $Fe(NO)_3(\eta^1\text{-}PF_6)$ (1). Treatment of $Fe(NO)_3Cl$ with 1 equiv of $[Ag][PF_6]$ in CH_2Cl_2, in a polypropylene vial, affords green solutions of $Fe(NO)_3(\eta^1\text{-}PF_6)$ (**1**) (eq 1)

$$Fe(NO)_3Cl + [Ag][PF_6] \rightarrow Fe(NO)_3(\eta^1\text{-}PF_6)\ (\mathbf{1}) + AgCl \quad (1)$$

Dark green fibrous needles of **1** can be isolated in 39% yield from CH_2Cl_2/hexanes solutions. The use of plastic reaction vessels is preferred over glass for this metathesis reaction since PF_6^- reacts with glass in the presence of trace amounts of water (vide infra). Complex **1** can also be synthesized by reacting $[NO][PF_6]$ with excess iron filings in rigorously purified $MeNO_2$ at room temperature in a polypropylene vial (eq 2). By this method, green needles of **1** can be isolated in 30% yield by crystallization of the final reaction residue from CH_2Cl_2/hexanes. The two extra electrons needed to form the trinitrosyl product in this manner most likely come from the oxidation of iron. Consequently, we presume that a solvated species such as $[Fe^{II}(O_2NMe)_x][PF_6]_2$ is generated as a byproduct during the transformation summarized by eq 2

$$2\ Fe + 3\ [NO][PF_6] + x MeNO_2 \rightarrow Fe(NO)_3(\eta^1\text{-}PF_6)\ (\mathbf{1}) + [Fe^{II}(MeNO_2)_x][PF_6]_2 \quad (2)$$

Solution IR spectral data for the $Fe(NO)_3$-containing complexes investigated during this study are collected in Table 1. Each spectrum exhibits the two ν(NO) absorptions expected for an $Fe(NO)_3$ fragment in a localized 3-fold symmetry environment, namely a weak vibration of a_1 symmetry and a strong vibration of e symmetry at lower wavenumbers.[16] The IR spectrum of authentic **1** in $MeNO_2$ solutions has a weak ν(NO) absorption at 1934 cm^{-1} and a strong absorption at 1822 cm^{-1}, whereas in CH_2Cl_2 these features appear at 1922 and 1810 cm^{-1}, respectively (Table 1). It is important to note that in nitromethane, **1** quickly reacts with the NaCl windows of the solution IR cell to generate $Fe(NO)_3Cl$, so an AgCl IR cell must be used to prevent this reaction from occurring. The shift of the ν(NO) frequencies to higher wavenumbers upon exchange of Cl^- for PF_6^- (Table 1) is consistent with the replacement of a reasonable electron-donating ligand (chloride) with a much poorer provider of electron density (hexafluorophosphate). Interestingly, the IR spectrum of **1** as a KBr pellet exhibits a weak ν(NO) absorption at 1907 cm^{-1} and a stronger one at 1795 cm^{-1}. These features are reminiscent of those displayed by $Fe(NO)_3Br$[16] and indicate that halide metathesis has occurred with the pellet material.

NMR studies of **1** have provided limited structural information since its only easily observed NMR nuclei are those contained in the PF_6^- ligand. Thus, the ^{19}F NMR spectrum of **1** in CD_2Cl_2 at 240 K consists of a broad doublet at 3.97 ppm (J_{PF} = 721 Hz), whereas its ^{31}P NMR spectrum in the same solvent consists of a broad septet at −149.6 ppm (J_{PF} = 728 Hz). Upon cooling to 200 K, the signal in the ^{19}F spectrum sharpens considerably, but still remains a doublet. Attempts to obtain the limiting spectrum by further cooling of the sample are hampered by the very low solubility of **1** in cold CD_2Cl_2. Unfortunately, the observed solution NMR spectra are consistent with a number of plausible processes. For instance, the PF_6^- ligand could be undergoing a rapid exchange between uncoordinated and coordinated modes, or it could be in the metal's coordination sphere, but the six fluorine sites could be undergoing rapid exchange that makes them appear equivalent on the NMR time scale.

We have also measured the solution conductivity of **1**. In $MeNO_2$, **1** exhibits a Λ_M of 54.5 $ohm^{-1}\cdot cm^2\cdot mol^{-1}$ at 23 °C and a Λ_M of 28.0 $ohm^{-1}\cdot cm^2\cdot mol^{-1}$ at −26 °C, for a 1.00 × 10^{-3} M solution. The expected molar conductivity for a 1:1 electrolyte in $MeNO_2$ is in the range of 75 to 95 $ohm^{-1}\cdot cm^2\cdot mol^{-1}$ at 25 °C,[17] somewhat higher than that exhibited by **1**, thereby suggesting that **1** may be partially dissociated in $MeNO_2$ at this concentration. More importantly, this result raises doubt about the formulation proposed by Herberhold and co-workers. Using the Herberhold formulation, $[Fe_2(NO)_6][PF_6]_2$, our Λ_M values become 109 $ohm^{-1}\cdot cm^2\cdot mol^{-1}$ at 23 °C and 56.0 $ohm^{-1}\cdot cm^2\cdot mol^{-1}$ at −26 °C, well below the range of a 1:2 electrolyte.[17] Herberhold and co-workers report an equivalent conductivity of 148 $ohm^{-1}\cdot cm^2\cdot mol^{-1}$ for $[Fe_2(NO)_6][PF_6]_2$ (−25.5 °C; 10^{-3} M solution). However, it is possible that they were actually measuring the conductivity of $[Fe(NO)_3(EtCN)][PF_6]$, because propionitrile is a commonly found impurity in commercially available $MeNO_2$ (vide infra).

Complex **1** is an exceedingly air- and moisture-sensitive solid. Once isolated from the final reaction mixture, it can only be handled at room temperature for short periods of time, but it is indefinitely stable below −20 °C. Solutions of **1** are only stable at low temperatures (−20 °C and below), and decomposition

(16) Jahn, A. *Z. Anorg. Allg. Chem.* **1959**, *301*.
(17) Geary, W. J. *Coord. Chem. Rev.* **1971**, *7*, 81−122.

is relatively rapid at room temperature. For instance, allowing an NMR sample of the compound to stand for several days at ambient temperatures results in its color changing from green to red-brown and the resonances disappearing from its ^{19}F NMR spectrum. Monitoring of similar solutions by IR spectroscopy shows the gradual diminution of the ν(NO) signals of **1** concomitant with the color change from green to brown. No ν(NO) absorptions are evident in the IR spectrum of the final solution. In addition, the rate of decomposition of **1** is greatly increased if its solutions are stored under vacuum.

Mass spectrometry of **1**, which could provide some additional evidence for formulating $Fe(NO)_3(\eta^1\text{-}PF_6)$ as either a monomer or a dimer, has so far failed to afford informative spectra, and to date we have been unable to grow crystals of **1** suitable for X-ray diffraction.

Synthesis and Characterization of $[Fe(NO)_3(EtCN)][PF_6]$ (2). Many attempts to grow X-ray quality crystals of **1** have been made, but only very thin needles, which did not diffract X-rays, could be obtained. In one crystallization, X-ray quality crystals were grown, but subsequent crystallographic analysis revealed the crystals to be $[Fe(NO)_3(EtCN)][PF_6]$ (**2**). The isolation of **2** during the attempted crystallization of **1** from $MeNO_2$ reflects the presence of EtCN, a common impurity in nitromethane.[18−20]

$$Fe(NO)_3(\eta^1\text{-}PF_6) + EtCN \rightarrow [Fe(NO)_3(EtCN)][PF_6]\ (\mathbf{2}) \quad (3)$$

Complex **2** can be made deliberately in good yields by treating $Fe(NO)_3(\eta^1\text{-}PF_6)$ with 1 equiv of EtCN in CH_2Cl_2 at room temperature (eq 3). If excess EtCN is used, very little of **2** is formed, and an oily orange-brown material is obtained instead. The identity of this material remains unknown, but monitoring of the reaction between **2** and excess EtCN in $MeNO_2$ by IR spectroscopy reveals the appearance of two new ν(NO) absorptions at 1814 and 1740 cm^{-1}. The spacing and intensity of these two peaks is diagnostic of a dinitrosyl species and may well indicate the formation of $[(EtCN)_2Fe(NO)_2][PF_6]$. However, all attempts to isolate and fully characterize this material have so far failed.

Crystals of **2** were found to crystallize in the space group $P\bar{1}$ as a four-component twin. The crystal structure of **2** consists of the packing of discrete cations and anions; the solid-state molecular structure of the cation portion is shown in Figure 1. The iron atom is at the center of a nearly perfect tetrahedral coordination geometry which exhibits an average N(nitrosyl)−Fe−N(nitrosyl) angle of 110.8°. The average Fe−N(nitrosyl) distance in the cation is 1.71 Å, whereas the average N−O distance is 1.14 Å, both parameters being typical for iron-nitrosyl linkages.[21] Surprisingly, each of the three Fe−NO links is slightly bent, displaying an average Fe−N−O angle of 169°. These Fe−N−O angles are much different than those found in $Mn(NO)_3(PPh_3)$, the only other structurally characterized trinitrosyl species, which contains linear NO ligands.[22] Finally, **2** displays an Fe−N(nitrile) distance of 1.979 (4) Å and a N−C distance of 1.139(5) Å, bond lengths that are comparable to those found in other EtCN complexes.[23]

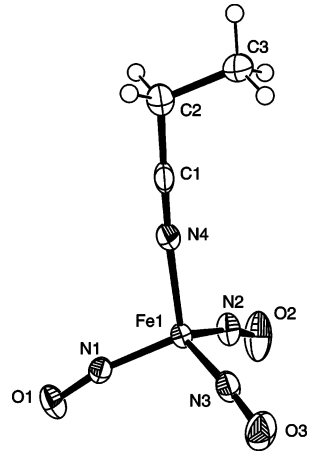

Figure 1. Solid-state molecular structure of the cation portion of $[Fe(NO)_3(EtCN)][PF_6]$ (**2**) with 50% probability ellipsoids shown. Selected interatomic distances (Å) and angles (deg): Fe1−N1 = 1.713(3), Fe1−N2 = 1.703(3), Fe1−N3 = 1.710(3), Fe1−N4 = 1.979(4), N1−O1 = 1.138(4), N2−O2 = 1.150(4), N3−O3 = 1.142(4), N4−C1 = 1.139(5), Fe1−N1−O1 = 168.9(3), Fe1−N2−O2 = 168.9(4), Fe1−N3−O3 = 168.8(4), Fe1−N4−C1 = 176.6(3), N1−Fe1−N2 = 110.5(1), N1−Fe1−N3 = 111.8(1), N2−Fe1−N3 = 110.2(1), N1−Fe1−N4 = 108.3(1), N2−Fe1−N4 = 108.2(2), N3−Fe1−N4 = 107.8(2), N4−C1−C2 = 178.8(4).

The IR spectrum of **2** as a Nujol mull exhibits a ν(CN) absorption at 2314 cm^{-1} and ν(NO) absorptions at 1949 and 1810 cm^{-1}. Its IR spectra in CH_2Cl_2 and $MeNO_2$ (Table 1) consist of two ν(NO) vibrations in intensity patterns identical to those exhibited by **1**. Indeed, the spectrum in $MeNO_2$ closely resembles that reported by Herberhold and co-workers for $[Fe_2(NO)_6][PF_6]_2$ in the same solvent.[24] We thus believe that their nitromethane was also probably contaminated with EtCN and that the solution IR spectrum that they report is in fact that of the EtCN adduct, $[Fe(NO)_3(EtCN)]^+$. In $MeNO_2$, as a 1.00 $\times$ 10^{-3} M solution, **2** exhibits a molar conductivity of 88.4 $ohm^{-1}\cdot cm^2\cdot mol^{-1}$ at 23 °C and 43.5 $ohm^{-1}\cdot cm^2\cdot mol^{-1}$ at −22 °C; these values are in accord with those expected for a 1:1 electrolyte.[17]

The ^1H NMR spectrum of **2** in CD_2Cl_2 at 183 K consists of two broad singlets at 1.41 and 2.94 ppm of relative intensities 3:2, which are attributable to the EtCN ligand. Upon warming of the solution, the resonance at 2.94 decreases in intensity, until at room temperature the ^1H NMR spectrum consists of a broad singlet centered at 1.55 ppm. At no temperature are signals due to free propionitrile evident, i.e., a triplet and a quartet in a 3:2 ratio. Also, when propionitrile is added to a CD_2Cl_2 solution of **2**, the resonance at 1.55 ppm increases in intensity and shifts slightly upfield to 1.37 ppm, but again no signals attributable to uncoordinated propionitrile are evident. Thus, the solution behavior of **2** is not straightforward, and the nitrile ligand may well be quite labile and exchanging quickly with free EtCN. Finally, unlike **1**, complex **2** appears to be reasonably thermally stable in solution at room temperature.

Isolation and Characterization of $[(ON)_3Fe(\mu\text{-}PO_2F_2)Fe(NO)_3][PF_6]$ (3). During one attempted synthesis of **1** by halide abstraction in a glass vessel, large dark green blocks were isolated, quite unlike the small needles usually obtained for **1**. Subsequent crystallographic analysis revealed these crystals to

(18) Bardin, J.-C. *Analusis* **1972**, *1*, 140−144.
(19) Coetzee, J. F.; Chang, T.-H. *Pure Appl. Chem.* **1986**, *58*, 1541−1545.
(20) Parrett, F. W.; Sun, M. S. *J. Chem. Educ.* **1977**, *54*, 448.
(21) Feltham, R. D.; Enemark, J. H. *Top. Stereochem.* **1981**, *12*, 155−215.
(22) Wilson, R. D.; Bau, R. *J. Organomet. Chem.* **1980**, *191*, 123−132.
(23) Rochon, F. D.; Melanson, R.; Thouin, E.; Beauchamp, A. L.; Bensimon, C. *Can. J. Chem.* **1996**, *74*, 144−152.
(24) The IR spectrum of $[Fe_2(NO)_6][PF_6]_2$ in $MeNO_2$ as reported in 1978 consists of a weak absorption at 1937 cm^{-1} and a strong absorption at 1828 cm^{-1}.

be $[(ON)_3Fe(\mu\text{-}PO_2F_2)Fe(NO)_3][PF_6]$ (**3**). Complex **3** crystallizes in the orthorhombic space group $Pna2_1$ and consists of discrete cation and anion portions. The bimetallic monocation consists of two pseudotetrahedral $Fe(NO)_3^+$ fragments bridged by a $PO_2F_2^-$ unit, for which an ORTEP diagram is shown in Figure 2. As in the structure of **2**, all six Fe−N−O linkages of **3** are significantly bent, with the Fe−N−O angles ranging from 159.4(9)° to 167.6(7)°. The Fe−N and N−O distances are also comparable in the two complexes, and the metrical parameters of the bridging PO_2F_2 ligand in **3** are consistent with other reported examples.[25]

Solution IR spectroscopy of **3** in both $MeNO_2$ and CH_2Cl_2 (Table 1) reflects the presence of the $Fe(NO)_3^+$ fragment, displaying a weak absorption at ca. 1930 cm^{-1} and a broad strong absorption at ca. 1820 cm^{-1} in both solvents. The ^{19}F NMR spectrum of **3** in CD_2Cl_2 at 240 K consists of a sharp doublet (J_{PF} = 724 Hz) at 3.86 ppm and a broad doublet (J_{PF} = 985 Hz) at −7.14 ppm in an intensity ratio of 6:2, respectively. The corresponding ^{31}P NMR spectrum displays a septet (J_{PF} = 705 Hz) at −149.6 ppm and a broad resonance at −5.8 ppm, in accord with the ^{19}F NMR data. Like those of **1**, solutions of **3** in CD_2Cl_2 are temperature sensitive, and after several hours at room temperature the color changes noticeably to a brown-orange shade and a brown powder is deposited on the walls of the NMR tube.

The bridging $PO_2F_2^-$ ligand in **3** probably results from the catalytic hydrolysis of PF_6^-, a well-known process[26,27] that is greatly facilitated by glass and needs very little H_2O to occur.[28] Hence, the formation of **3** is best represented by eq 4 below

$$2\ Fe(NO)_3Cl + 2\ [Ag][PF_6] + 2\ H_2O \rightarrow [(ON)_3Fe(\mu\text{-}PO_2F_2)Fe(NO)_3][PF_6]\ (\mathbf{3}) + 2\ AgCl + 4\ HF \quad (4)$$

Synthesis and Characterization of $Fe(NO)_3(\eta^1\text{-}BF_4)$ (4). Given the difficulty in obtaining a crystallographic analysis of **1**, we next attempted to form the related tetrafluoroborate salt, $Fe(NO)_3(\eta^1\text{-}BF_4)$, with the hope that it would be more amenable to characterization by X-ray diffraction. As expected, $Fe(NO)_3(\eta^1\text{-}BF_4)$ (**4**) can be synthesized by treating $Fe(NO)_3Cl$ with an equimolar amount of $[Ag][BF_4]$ in CH_2Cl_2 at room temperature (eq 5)

$$Fe(NO)_3Cl + [Ag][BF_4] \rightarrow Fe(NO)_3(\eta^1\text{-}BF_4)\ (\mathbf{4}) + AgCl \quad (5)$$

Complex **4** can be isolated in 34% yield from CH_2Cl_2/pentane as a green microcrystalline powder. It can also be formed by the reaction of $[NO][BF_4]$ with excess iron powder in $MeNO_2$ at room temperature under an atmosphere of NO (1 atm) (eq 6). The yield, however, is quite low (7%), and unlike the formation of **1** by eq 2, the formation of **4** by eq 6 requires the use of an NO atmosphere, otherwise an intractable green oil is the only material isolated.

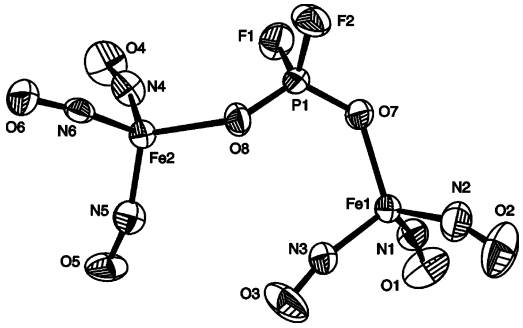

Figure 2. Solid-state molecular structure of the cation portion of $[(ON)_3Fe(\mu\text{-}PO_2F_2)Fe(NO)_3][PF_6]$ (**3**) with 50% probability ellipsoids shown. Selected interatomic distances (Å) and angles (deg): Fe1−N1 = 1.697(9), Fe1−N2 = 1.72(1), Fe1−N3 = 1.683(6), Fe2−N4 = 1.684(9), Fe2−N5 = 1.708(8), Fe2−N6 = 1.721(7), N1−O1 = 1.15(1), N2−O2 = 1.15(1), N3−O3 = 1.151(8), N4−O4 = 1.15(1), N5−O5 = 1.16(1), N6−O6 = 1.151(8), Fe1−O7 = 1.969(5), Fe2−O8 = 1.976(6), P1−O7 = 1.455(5), P1−O8 = 1.465(5), P1−F1 = 1.519(8), P1−F2 = 1.533(7), Fe1−N1−O1 = 159.4(9), Fe1−N2−O2 = 161(1), Fe1−N3−O3 = 167.6(7), Fe2−N4−O4 = 165.2(9), Fe2−N5−O5 = 163.6(7), Fe2−N6−O6 = 159.4(9), O7−P1−O8 = 120.2(3), F1−P1−F2 = 98.6(3).

$$2\ Fe + 3\ [NO][BF_4] + x MeNO_2 \rightarrow Fe(NO)_3(\eta^1\text{-}BF_4)\ (\mathbf{4}) + [Fe^{II}(MeNO_2)_x][BF_4]_2 \quad (6)$$

Not surprisingly, the IR spectra of **4** in $MeNO_2$ and CH_2Cl_2 are almost identical to those of **1** (Table 1). The ^{19}F NMR spectrum of **4** in CD_2Cl_2 at 240 K consists of a broad singlet at −99.4 ppm that sharpens slightly upon cooling to 200 K. As for **1** (vide supra), these results are consistent with a number of different solution behaviors, including the partial dissociation of the BF_4^- anion or the rapid exchange of the four F sites of a η^1-bound tetrafluoroborate anion.

Solutions of **4**, like those of **1**, are very temperature sensitive. Upon standing at room temperature, they change color from yellow-green to orange-brown with the concomitant deposition of an intractable brown powder. However, both solid **4** and its solutions can be stored at −30 °C for long periods with no decomposition being evident.

Crystals of $Fe(NO)_3(\eta^1\text{-}BF_4)$ suitable for X-ray diffraction were grown slowly from a CH_2Cl_2/pentane solution stored at −30 °C for several months. Crystallographic analysis has confirmed the monomeric nature of **4**, and its solid-state molecular structure is shown in Figure 3. Solid-state metrical parameters for **4** are collected in Table 2. The iron center in **4** is in a pseudotetrahedral environment with three coordination sites being occupied by nitrosyl ligands and the fourth by a BF_4^- ligand coordinated in a monodentate fashion via an F→Fe bond. The Fe(1)−F(1) distance is 1.977(2) Å which is in the midrange of typical Fe−F bonds (1.86−2.25 Å).[29] The average Fe−N bond length in **4** is 1.72 Å, whereas the average N−O bond length is 1.15 Å, both parameters being very similar to those extant in the cation of **2**. Also similar to the structure of $[Fe(NO)_3(EtCN)]^+$, all three Fe−N−O linkages in **4** are distinctly bent away from the BF_4^- ligand, with the average bond angle being 163°. Furthermore, the three nitrosyl ligands

(25) Gusev, O. V.; Kalsin, A. M.; Peterleitner, M. G.; Petrovskii, P. V.; Lyssenko, K. A.; Akhmedov, N. G.; Bianchini, C.; Meli, A.; Oberhauser, W. *Organometallics* **2002**, *21*, 3637−3649.
(26) Jeffery, J. C.; Jelliss, P. A.; Lebedev, V. N.; Stone, F. G. A. *Organometallics* **1996**, *15*, 4737−4746.
(27) Stoop, R. M.; Bauer, C.; Setz, P.; Wörle, M.; Wong, T. Y. H.; Mezzetti, A. *Organometallics* **1999**, *18*, 5691−5700.
(28) Fernández-Galán, R.; Manzano, B. R.; Otero, A.; Lanfranchi, M.; Pellinghelli, M. A. *Inorg. Chem.* **1994**, *33*, 2309−2312.
(29) A search of the Cambridge Structural Database (Version 5.24) found 52 compounds with Fe−F bonds of which 46 (88%) had Fe−F bond lengths between 1.86 and 2.25 Å.

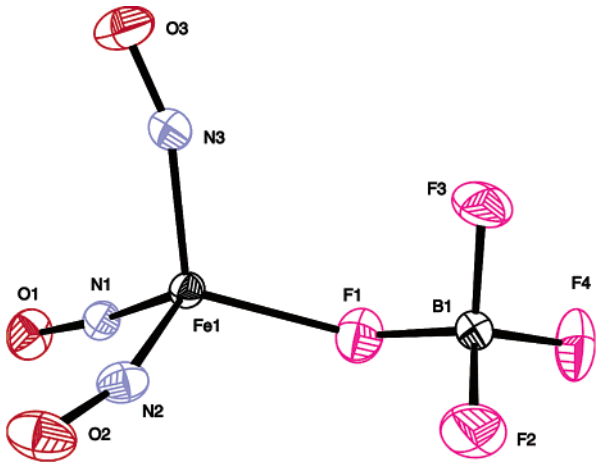

Figure 3. Solid-state molecular structure of $Fe(NO)_3(\eta^1\text{-}BF_4)$ (**4**) with 50% probability ellipsoids shown.

Table 2. Selected Bond Lengths (Å) and Angles (deg) for the Experimentally Determined Structure of $Fe(NO)_3(\eta^1\text{-}BF_4)$ **4**, and the Optimized Structures of $Fe(NO)_3(\eta^1\text{-}BF_4)$ at the B3LYP/LANL2DZ and B3LYP/6-311+G(2d,2p) Levels of Theory

X-ray crystallography		B3LYP/LANL2DZ		B3LYP/6-311+G(2d,2p)	
bond lengths					
Fe1−N1	1.711(2)	Fe1−N2	1.6762	Fe1−N2	1.6808
Fe1−N2	1.708(2)	Fe1−N4	1.6747	Fe1−N4	1.6761
Fe1−N3	1.735(2)	Fe1−N6	1.6749	Fe1−N6	1.6758
N1−O1	1.155(3)	N2−O3	1.1876	N2−O3	1.1447
N2−O2	1.147(3)	N4−O5	1.1790	N4−O5	1.1374
N3−O3	1.151(3)	N6−O7	1.1791	N6−O7	1.1378
Fe1−F1	1.977(2)	Fe1−F8	1.9572	Fe1−F8	1.9524
bond angles					
Fe1−N1−O1	165.4(2)	Fe1−N2−O3	169.29	Fe1−N2−O3	162.46
Fe1−N2−O2	161.4(2)	Fe1−N4−O5	173.33	Fe1−N4−O5	166.91
Fe1−N3−O3	161.9(2)	Fe1−N6−O7	173.28	Fe1−N6−O7	166.80
Fe1−F1−B1	124.7(2)	Fe1−F8−B9	118.29	Fe1−F8−B9	117.44
N1−Fe1−N2	106.5(1)	N2−Fe1−N4	113.12	N2−Fe1−N4	109.49
N1−Fe1−N3	109.9(1)	N2−Fe1−N6	113.15	N2−Fe1−N6	109.50
N2−Fe1−N3	106.6(1)	N4−Fe1−N6	112.55	N4−Fe1−N6	108.84
N1−Fe1−F1	109.74(9)	N2−Fe1−F8	110.33	N2−Fe1−F8	113.07
N2−Fe1−F1	111.27(9)	N4−Fe1−F8	103.34	N4−Fe1−F8	107.86
N3−Fe1−F1	112.65(9)	N6−Fe1−F8	103.40	N6−Fe1−F8	108.00

are bound asymmetrically. The two NO ligands proximal to the BF_3 fragment display Fe−N−O angles of 161.4(2)° (for Fe1−N2−O2) and 161.9(2)° (for Fe1−N3−O3), whereas the NO ligand distal to the BF_3 fragment exhibits an Fe−N−O angle of 165.4(2)°. In addition, the BF_3 fragment is in an eclipsed configuration with respect to the $Fe(NO)_3$ group. The results of this crystallographic analysis of **4** provide the strongest evidence yet that the original formulation of the green material isolated in 1978 as $[Fe_2(NO)_6][PF_6]_2$, is probably incorrect and that the solid-state molecular structure of **1** is $Fe(NO)_3(\eta^1\text{-}PF_6)$.

Solid-State Molecular Structure of $Fe(NO)_3Cl$. The interesting intramolecular metrical parameters of the $Fe(NO)_3$-containing entities in complexes **2**, **3**, and **4** motivated us to determine the solid-sate molecular structure of $Fe(NO)_3Cl$, their parent compound. $Fe(NO)_3Cl$ was first synthesized in 1940,[30] yet to the best of our knowledge, no crystal structure data for this compound exists. Crystals of $Fe(NO)_3Cl$ can be grown from hexanes by allowing NO(g) to diffuse slowly through a solution of $[Fe(NO)_2Cl]_2$.[31] $Fe(NO)_3Cl$ crystallizes in the trigonal space group $P6_3mc$ in which it contains a crystallographically imposed 3-fold axis making all three nitrosyl groups equivalent. The solid-state molecular structure of $Fe(NO)_3Cl$ is shown in Figure 4. The most striking feature of its solid-state structure involves its bent Fe−N−O linkages of 161.5(4)°. The Fe−N and N−O bond lengths of 1.702(4) Å and 1.152(5) Å, respectively, are common for iron nitrosyls and similar to those extant in **4**. The molecular geometry of $Fe(NO)_3Cl$ is slightly distorted away from a perfect tetrahedron, with N1−Fe1−N1* being 106.5(2)° and N1−Fe1−Cl1 being 112.3(2)°. This is in contrast to the structure of $Mn(NO)_3(PPh_3)$ which exhibits much larger N−M−N angles (av. 114.7°).[22]

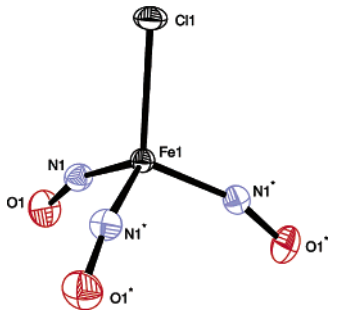

Figure 4. Solid-state molecular structure of $Fe(NO)_3Cl$ with 50% probability ellipsoids. Interatomic distances (Å) and angles (deg): Fe1−N1 = 1.702(4), N1−O1 = 1.152(5), Fe1−Cl1 = 2.252(2), Fe1−N1−O1 = 161.5(4), N1−Fe1−N1* = 106.5(2), N1−Fe1−Cl1 = 112.3(2).

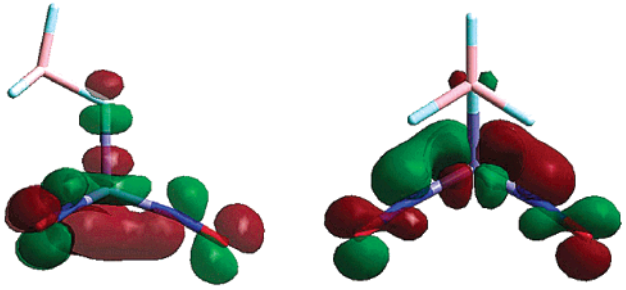

Figure 5. Representations of the HOMO (left) and the HOMO-1 (right) of $Fe(NO)_3(\eta^1\text{-}BF_4)$ as determined at the B3LYP/LANL2DZ level of theory. The views illustrate the interaction of the Fe orbitals, which are predominantly d in character, with the NO π^* orbitals.

Theoretical Investigations of $Fe(NO)_3(\eta^1\text{-}BF_4)$ (4). DFT calculations have been performed on $Fe(NO)_3(\eta^1\text{-}BF_4)$ in an attempt to discern the factors responsible for its nonlinear Fe−N−O linkages. Using the LANL2DZ basis set, a geometry optimization reproduces the key features of the experimentally determined structure (vide supra), including an effective C_S symmetry, the approximately tetrahedral Fe−F−B angle, an "eclipsed" configuration of the BF_3 and $Fe(NO)_3$ groups, and bent nitrosyl ligands (Table 2). However, the optimized structure shows one Fe−N−O angle to be slightly more acute than the other two, rather than the observed reverse, and the degree of NO bending is underestimated, in that the optimized structure shows Fe−N−O angles of 173°, 173°, and 169°, on average about 9° more obtuse that those observed in the solid-state molecular structure. A pictorial representation of the HOMO and the HOMO-1 orbitals for $Fe(NO)_3(\eta^1\text{-}BF_4)$ calculated at this level of theory is shown in Figure 5. Use of the larger 6-311+G(2d,2p) basis set gives much better agreement with experimental observations, the calculated Fe−N−O angles being 167°, 167°, and 162° (Table 2). These calculations indicate that

(30) Hieber, W.; Nast, R. *Z. Anorg. Allg. Chem.* **1940**, *244*, 23−47.
(31) Herberhold, M.; Klein, R.; Alt, H. G. *Isr. J. Chem.* **1977**, *15*, 206−209.

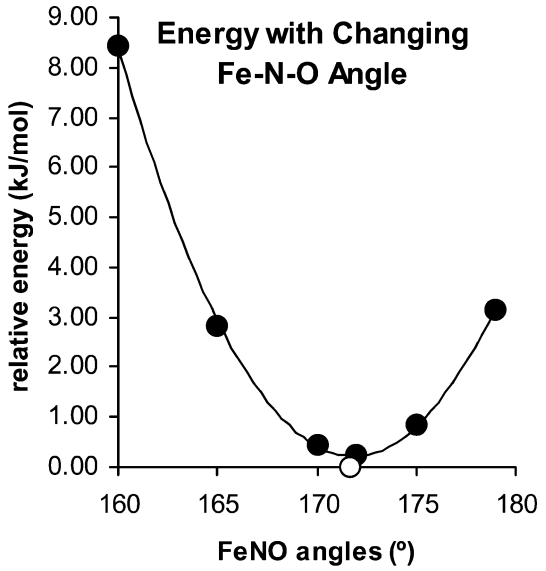

Figure 6. Relative total energy of $Fe(NO)_3(\eta^1\text{-}BF_4)$ as a function of Fe−N−O angle. The open circle represents the unrestricted optimized structure of $Fe(NO)_3(\eta^1\text{-}BF_4)$ in which the three Fe−N−O angles are allowed to be independent.

the bent Fe−N−O links do indeed have an electronic origin and need not be attributed to other factors such as packing forces in the crystal.

In that the much greater computational demands of the larger basis set rendered its use for a more detailed study impractical, and because the LANL2DZ basis set does qualitatively reproduce the nonlinear arrangement of the nitrosyl ligands, the latter basis set was employed in a series of partial optimizations to elucidate the origin of this nonlinearity. Lowest-energy structures were determined with all three Fe−N−O angles being held at identical values of 160°, 165°, 170°, 172° 175°, and 179° (Figure 6). Variation of the Fe−N−O angle represents a very shallow energy well, with the calculated global energy minimum being only 3.16 kJ/mol below a structure with three (nearly) linear nitrosyl groups and 8.42 kJ/mol below that with Fe−N−O angles of 160°. Indeed, the curve is a perfect parabolic function ($R^2 = 0.9996$) with a minimum at 171.95°. The calculated structure with three angles of 172° is only 0.24 kJ/mol above the unrestricted optimized structure, which exhibits an average Fe−N−O angle of 171.7° (represented by the open circle in Figure 6).

An examination of the frontier-orbital energies of these partially optimized structures reveals clear trends with variation of the Fe−N−O angle. In a C_{3v} symmetric $XFe(NO)_3$ complex, the five metal d-orbitals transform as a_1 (d_{z^2}), e (d_{xy} and $d_{x^2-y^2}$), and e (d_{xz} and d_{yz}), whereas the six combinations of NO π-symmetry orbitals have a_1 and e symmetry (parallel to the z axis), and a_2 and e symmetry (orthogonal to z).[32] The a_2 combination is nonbonding, but the others can form π-interactions to varying degrees. The nearly tetrahedral angles in the complex mean that the Fe−N bonds lie almost perfectly in the nodal cone of the d_{z^2} orbital. Thus, when the Fe−N−O angles are linear, the a_1 set has maximum overlap with the d_{z^2} orbital, and this bonding interaction represents the HOMO of the compound (which is also π-antibonding with respect to the X group). Bending of the NO ligand away from the X ligand reduces this π-interaction, and a corresponding increase in the energy of the HOMO results (Figure 7a). Such an effect seems

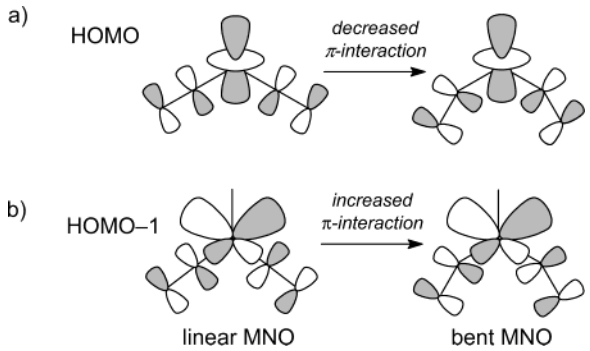

Figure 7. (a) Qualitative pictorial representation of the decreased π interaction upon M−N−O bending for the HOMO. (b) Qualitative pictorial representation of the increased π interaction upon M−N−O bending for the HOMO-1.

to destabilize the complex, suggesting that Fe−N−O bending should be unfavorable. However, the same distortion causes an increased overlap with one set of e symmetry orbitals, interactions that form the HOMO-1 and HOMO-2 in the complex (Figure 7b). In the linear case, the tetrahedral framework points the lobe of the metal d−p hybrid directly toward the nodal plane of the NO π^* orbital, resulting in poor overlap. Upon bending this is no longer the case, and the overlap increases. As a result, the HOMO-1 and HOMO-2 both decrease in energy as the Fe−N−O angle become more acute, a feature that stabilizes the compound (Figure 8). In effect, the nitrosyl ligands bend due to the presence of nondegenerate sets of π-overlaps, parallel and orthogonal to the z-axis, the latter of which involves twice as many interactions. The compound trades energy of the HOMO to stabilize the two orbitals below it, thereby resulting in a net lowering of energy for the system. This effect is further enhanced in the unrestricted optimization in which the three angles need no longer be equal, represented again by open shapes on the graph (Figure 8). The HOMO is higher, while HOMO-1 and HOMO-2 are still lower in energy than in the restricted cases, so that the unequal nature of the three Fe−N−O groups represents a further stabilizing influence. Gratifyingly, this calculated structure closely parallels the experimentally determined structure of $Fe(NO)_3(\eta^1\text{-}BF_4)$ (vide supra).

A second series of partial optimizations explicitly demonstrates that a similar enhanced π-overlap cannot be gained simply by a variation of the F−Fe−N angles. Structures were minimized with the Fe−N−O angles at 179° and three identical F−Fe−N angles of 95°, 100°, 105°, 110°, and 115°. The partially optimized structure with linear NO groups has an average F−Fe−N angle of 103°. The computational results are shown in Figure 9, and they reveal a very significant destabilization of the complex with any deviation of the F−Fe−N angle from ca. 103°. In other words, changes in the $Fe(NO)_3$ cone angle at the metal center do not stabilize the complex.

(32) The C_3 axis is taken as z. This scheme represents a small oversimplification, in that mixing occurs among the various sets of e-symmetry orbitals, which includes p_x and p_y. Thus, a description of the metal wave functions as single canonical atomic orbitals is not wholly accurate. The situation is further complicated in the reduced (approximately C_S) symmetry observed in $F_3BFFe(NO)_3$, in that greater mixing among d-orbitals takes place, and the orbitals in the e sets no longer remain perfectly degenerate. The actual molecular orbitals that result are no longer so easily described in terms of specific d-orbitals. Perhaps more fundamentally, the Kohn−Sham orbitals used in DFT calculations are inherently different wave functions than those used in a pure Hartree−Fock approach. Nevertheless, examination of the shape of calculated DFT eigenfucntions shows that the general symmetry and nature of the frontier orbital overlaps are correctly captured by this simpler qualitative picture.

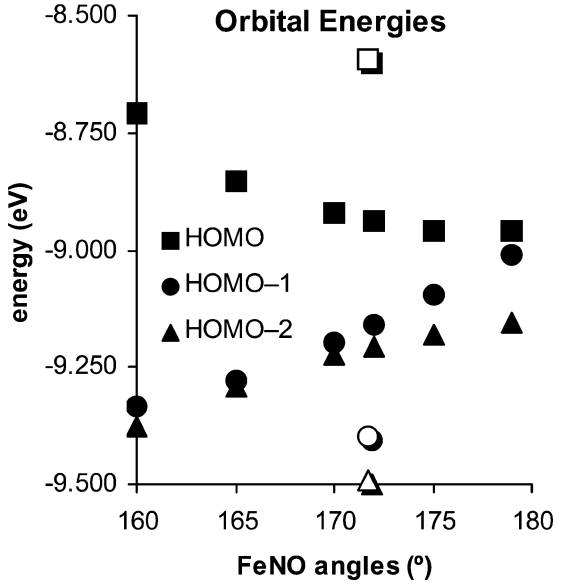

Figure 8. Orbital energies of HOMO, HOMO-1, and HOMO-2 in $Fe(NO)_3(\eta^1\text{-}BF_4)$ as a function of Fe−N−O angle. The open shapes represent the calculated structure in which the three Fe−N−O angles are allowed to be independent.

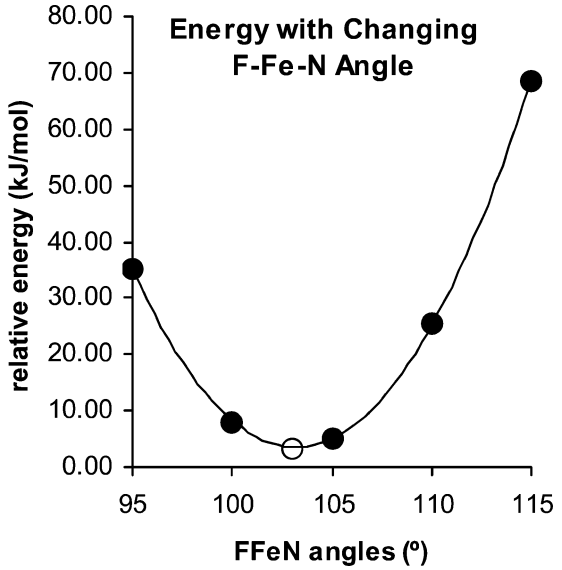

Figure 9. Relative total energy of $Fe(NO)_3(\eta^1\text{-}BF_4)$ as a function of F−Fe−N angle, with Fe−N−O held at 179°. The open circle represents the partially optimized structure with linear NO ligands in which the three F−Fe−N angles are allowed to optimize independently and with an energy of 3.16 kJ/mol above the fully optimized structure.

To put our observations in context, it had previously been suggested that $Mn(NO)_3(CO)$ might have distinctly nonlinear M−N−O groups of the type observed in this study with the $Fe(NO)_3$ systems.[33] However, this prediction has not been confirmed experimentally.[22] Indeed, tetrahedral or octahedral 18e nitrosyl complexes almost always contain linear M−N−O linkages, and exceptions are extremely rare.[21] Slight deviations from linearity in mononitrosyl complexes are sometimes found for species with asymmetric ligand fields, because it was demonstrated some time ago that the two d-π^* interactions involved in the M−NO bonding need not be identical.[34] In other words, in a low symmetry complex one should expect a difference in the occupation of the two π^* orbitals and consequently nonlinear M−N−O groups. However, this effect is normally quite small. Tetrahedral dinitrosyl complexes are also known to occasionally exhibit nonlinear nitrosyl ligands, and this phenomenon has been explained by Summerville and Hoffmann.[35] Interestingly, their rationalization is very similar to the one we proffer for our $Fe(NO)_3$-containing complexes. Finally, it may be noted that the second-order Jahn−Teller effect has been invoked to explain the bending of nitrosyl ligands,[33] as occurs in the case of $Rh(PPh_3)_3(NO)$ which has a Rh−N−O angle of ca. 157° in the solid state.[21,36] However, as we have outlined in the preceding paragraphs, such an effect need not be invoked to account for the molecular structures of our iron trinitrosyl complexes.

Epilogue

We can now report as a result of our investigations that the binary iron nitrosyl complex originally reported by Herberhold and co-workers as $[Fe_2(NO)_6][PF_6]_2$ is, in fact, $Fe(NO)_3(\eta^1\text{-}PF_6)$, a monometallic, pseudotetrahedral trinitrosyl complex. In other words, the 16e $[Fe(NO)_3]^+$ cation preferentially coordinates its counteranion rather than associating with itself to permit the iron center to attain the favored 18e configuration. Furthermore, we have demonstrated that M−NO bending is ubiquitous in this class of compounds as each nitrosyl ligand in each of the four structurally characterized complexes is bent by ca. 15°. There is no doubt that this bending is electronic in origin and is not a crystal-packing phenomenon. Our theoretical investigation of this system has demonstrated that upon bending, the HOMO is destabilized relative to the linear case, yet at the same time the HOMO-1 and the HOMO-2 are significantly stabilized, and this stabilization is sufficient to counteract the increase in the energy of the HOMO. The overall result is that the structure with the bent NO ligands is the lowest in energy.

Our initial studies of $Fe(NO)_3(\eta^1\text{-}PF_6)$ and related complexes have also shed some light on the characteristic chemistry of the base-stabilized $[Fe(NO)_3]^+$ cation, but some questions remain unanswered. Our future investigations in this area will be designed to further elucidate the solution behavior of $[Fe(NO)_3]^+$. For instance, we intend to determine whether $[(ON)_3Fe(L)]^+$ complexes, where L is a π-acid ligand, also exhibit nonlinear Fe−N−O linkages or whether they become linear as in $Mn(NO)_3(PPh_3)$. In addition, we shall explore the possibility of isolating $[Fe(NO)_3]^+$, unsolvated and uncoordinated by any ligand, through judicious use of a very weakly coordinating anion. Finally, we intend to ascertain whether reduction of these base-stabilized $Fe(NO)_3$ complexes affords binary nitrosyls such as $Fe_2(NO)_6$ or $[Fe(NO)_3]^{2-}$ and whether the preparative methods used to synthesize these iron nitrosyl species may be employed for the synthesis of binary nitrosyl complexes of other transition metals. We shall report the results of these investigations in due course.

Experimental Section

All reactions and subsequent manipulations were performed under anaerobic and anhydrous conditions either under high vacuum or an atmosphere of prepurified dinitrogen or argon. General procedures routinely employed in these laboratories have been described in detail

(33) Enemark, J. H.; Feltham, R. D. *Coord. Chem. Rev.* **1974**, *13*, 339−406.
(34) Kettle, S. F. A. *Inorg. Chem.* **1965**, *4*, 1661−1663.
(35) Summerville, R. H.; Hoffmann, R. *J. Am. Chem. Soc.* **1976**, *98*, 7240−7254.
(36) Kaduk, J. A.; Ibers, J. A. *Isr. J. Chem.* **1977**, *15*, 143−148.

previously.[37] $MeNO_2$ was recrystallized from Et_2O four times, stored over activated 4Å sieves, and then distilled.[18−20] CH_2Cl_2 was distilled from CaH_2. EtCN was dried over 4Å molecular sieves. $[NO][BF_4]$, $[NO][PF_6]$, $[Ag][BF_4]$, $[Ag][PF_6]$, and Fe were purchased from Strem and used as received. $Fe(NO)_3Cl$ was synthesized by the published procedure.[31] NMR spectra were recorded on either Bruker AMX 500 or AVA 300 spectrometers. ^1H and ^{13}C spectra are referenced to external $SiMe_4$ using the residual protio solvent peaks as internal standards (^1H experiments) or the characteristic resonances of the solvent nuclei (^{13}C experiments). ^{31}P spectra are referenced to external 85% H_3PO_4, whereas ^{19}F spectra are referenced to external trifluoroacetic acid. IR spectra were recorded on a BOMEM MB-100 FT-IR spectrometer or a Mattson Genesis FT-IR spectrometer. Conductivity measurements were performed using a VWR 2052 Conductivity Meter equipped with a Au dip cell. Elemental analyses were performed on a Carlo Erba EA1108 elemental analyzer by Mr. Minaz Lakha of this Department. Generally, the analyses were acceptable for carbon and hydrogen content, but they were consistently low for nitrogen. This phenomenon occurred for all the iron-trinitrosyl complexes isolated during this work, including $Fe(NO)_3Cl$, and it suggests an inherent difficulty in fully oxidizing the $Fe(NO)_3$ fragment to determine its N content accurately.

$Fe(NO)_3(\eta^1\text{-}PF_6)$ (1). Method A. A polypropylene vial was charged with $Fe(NO)_3Cl$ (0.087 g, 0.48 mmol) and $[Ag][PF_6]$ (0.125 g, 0.49 mmol). CH_2Cl_2 (3 mL) was added, and the mixture was stirred for 5 h. The resulting suspension was filtered through diatomaceous earth (2. × 0.5 cm) supported on glass wool to obtain a clear yellow-brown filtrate. The diatomaceous earth column was rinsed with CH_2Cl_2 (1 mL). To the combined filtrates were added hexanes (4 mL), and the solution was stored at −30 °C for several days to induce the deposition of green crystals of **1** (0.055 g, 39%). Anal. Calcd for $F_6FeN_3O_3P$: N, 14.45. Found: N, 13.63. IR (CH_2Cl_2): ν(NO) 1922 (w), 1810 (s), cm^{-1} IR ($MeNO_2$): ν(NO) 1934 (w), 1822 (s) cm^{-1}. NMR: ^{31}P (CD_2Cl_2, 121 MHz, 240 K) δ −149.6 (septet, J_{PF} = 728 Hz); ^{19}F (CD_2Cl_2, 282 MHz, 240 K) δ 3.97 (d, J_{PF} = 721 Hz). Λ_M (−26 °C, $MeNO_2$, 1.00 × 10^{-3} M): 28.0 $ohm^{-1}\cdot cm^2\cdot mol^{-1}$; Λ_M (23 °C, $MeNO_2$, 1.00 × 10^{-3} M): 54.5 $ohm^{-1}\cdot cm^2\cdot mol^{-1}$.

Method B. A polypropylene vial was charged with Fe filings (0.372 g, 6.7 mmol) and $[NO][PF_6]$ (0.207 g, 1.2 mmol). $MeNO_2$ (3 mL) was added, and the mixture was stirred at room temperature for 72 h. The $MeNO_2$ was removed from the final mixture in vacuo, and the remaining solids were extracted into CH_2Cl_2 (6 × 1 mL) and filtered though diatomaceous earth (2 × 0.5 cm) supported on glass wool to obtain green filtrates. To the combined filtrates were added hexanes (6 mL), and the resulting solution was stored at −30 °C for several days to induce the deposition of green crystals of **1** (0.034 g, 30%).

$[Fe(NO)_3(EtCN)][PF_6]$ (2). To a rapidly stirred solution of $Fe(NO)_3(\eta^1\text{-}PF_6)$ (**1**) (0.091 g, 0.31 mmol) in CH_2Cl_2 (20 mL) was added EtCN (22 μL, 0.31 mmol). The solution was stirred for 20 min and was then layered with pentane (20 mL) and stored at −30 °C for several days to induce the deposition of green crystals of **2** (0.055 g, 51%). Anal. Calcd for $C_3H_5F_6FeN_4O_3P$: C, 10.42; H, 1.46; N, 16.20. Found: C, 10.62; H, 1.30; N, 14.17 (trial 1); C, 10.60; H, 1.52; N, 14.66 (trial 2); C, 10.52; H, 1.73; N, 13.14 (trial 3). IR (Nujol): ν(CN) 2314 (w), ν(NO) 1949 (w), 1810 (s br) cm^{-1}. IR (CH_2Cl_2): ν(NO) 1939 (w), 1836 (s) cm^{-1}. IR ($MeNO_2$): ν(NO) 1942 (w), 1831 (s) cm^{-1}. NMR: ^1H (CD_2Cl_2, 500 MHz, 183K) δ 1.41 (br s, 3H, CH_3), 2.94 (br s, 2H, CH_2); $^{13}C\{^1H\}$ (CD_2Cl_2, 125 MHz, 183 K) δ 9.1 (CH_3), 12.4 (CH_2), 138.0 ($NCCH_2$); ^{31}P (CD_2Cl_2, 121 MHz, 185 K) δ −143.8 (septet, J_{PF} = 713 Hz); ^{19}F (CD_2Cl_2, 282 MHz, 185 K) δ 3.82 (d, J_{PF} = 714 Hz). Λ_M (−22 °C, $MeNO_2$, 1.00 × 10^{-3} M): 43.5 $ohm^{-1}\cdot cm^2\cdot mol^{-1}$; Λ_M (23 °C, $MeNO_2$, 1.00 × 10^{-3} M): 88.4 $ohm^{-1}\cdot cm^2\cdot mol^{-1}$.

$[Fe(NO)_3(\mu\text{-}PO_2F_2)Fe(NO)_3][PF_6]$ (3). A glass Schlenk tube was charged with $[Fe(NO)_2Cl]_2$ (0.301 g, 0.99 mmol), and CH_2Cl_2 (20 mL) was added to obtain a deep red solution. NO gas was then slowly bubbled through the solution for 20 min during which time the solution became deep brown. $[Ag][PF_6]$ (0.510 g, 2.02 mmol) was added via a powder funnel under a strong purge of argon, and the resulting suspension was stirred for 5 d. The mixture was then filtered though diatomaceous earth (2 × 2 cm) supported on a medium porosity frit to obtain a yellow-brown filtrate. The diatomaceous earth column was washed with CH_2Cl_2 (10 mL), and the volume of the combined filtrates was reduced in vacuo to 10 mL. The final solution was stored at −30 °C for 24 h to induce the deposition of a brown powder, which was removed by filtration though a column of (2 × 2 cm) and discarded. Pentane (15 mL) was added to the filtrate, and the mixture was stored at −30 °C for 24 h resulting in the deposition of more brown powder. Again, the powder was removed by filtration though a diatomaceous earth column (2 × 2 cm) and discarded. Finally, hexanes (10 mL) were added to the filtrate, and the mixture was stored at −30 °C for 72 h to induce the deposition of green crystals of **3** (0.072 g, 13.5%). Anal. Calcd for $F_8Fe_2N_6O_8P_2$: N, 15.63. Found: N, 13.29. IR ($MeNO_2$): ν(NO) 1932 (w), 1822 (s) cm^{-1}. IR (CH_2Cl_2): ν(NO) 1923 (w), 1813 (s) cm^{-1}. NMR: ^{31}P (CD_2Cl_2, 121 MHz, 240 K) δ −149.6 (br septet, J_{PF} = 705 Hz), −5.8 (br s); ^{19}F (CD_2Cl_2, 282 MHz, 240 K) δ 3.86 (6F, d, J_{PF} = 724 Hz), −7.14 (2F, br d, J_{PF} = 985 Hz).

$Fe(NO)_3(\eta^1\text{-}BF_4)$ (4). Method A. A glass Schlenk tube was charged with $[Fe(NO)_2Cl]_2$ (0.286 g, 0.95 mmol), and CH_2Cl_2 (15 mL) was added to obtain a deep red solution. NO gas was then slowly bubbled through the solution for 20 min whereupon the solution became deep brown. Under a strong purge of argon $[Ag][BF_4]$ (0.370 g, 1.9 mmol) was added via a powder funnel, and the resulting suspension was stirred for 48 h. The mixture was then filtered though diatomaceous earth (2 × 2 cm) supported on a medium porosity frit to obtain a yellow-brown filtrate. The diatomaceous earth column was washed with CH_2Cl_2 (10 mL), and pentane (15 mL) was carefully layered onto the combined CH_2Cl_2 filtrates. Storage of the resulting mixture at −30 °C for 72 h resulted in the deposition of **4** as a green powder (0.15 g, 34%). Anal. Calcd for $BF_4FeN_3O_3$: N, 18.06. Found: N, 15.72. IR ($MeNO_2$): ν(NO) 1934 (w), 1817 (s) cm^{-1}. IR (CH_2Cl_2): ν(NO) 1922 (w), 1814 (s) cm^{-1}. NMR: ^{19}F (CD_2Cl_2, 282 MHz, 240 K) δ −99.4.

Method B. A glass reaction bomb was charged with Fe filings (0.667 g, 12.4 mmol) and $[NO][BF_4]$ (0.165 g, 1.41 mmol). $MeNO_2$ (10 mL) was added, and the resulting mixture was stirred for 48 h under an atmosphere of NO(g) (1 atm). The solvent was removed from the final mixture in vacuo to obtain a green oil which was then dissolved in CH_2Cl_2 (10 mL) and filtered though diatomaceous earth (2 × 2 cm) supported on a medium porosity frit to obtain a green filtrate. The diatomaceous earth column was washed with CH_2Cl_2 (2 × 10 mL), and the combined filtrates were reduced in volume in vacuo to 10 mL. Pentane (30 mL) was carefully layered onto the CH_2Cl_2 solution, and the mixture was stored at −30 °C for 24 h to induce the deposition of green oil. The supernatant solution was decanted, and the oil was redissolved in CH_2Cl_2 (3 mL) to obtain a green solution. This solution was layered with pentane (2 mL), and the mixture was allowed to stand at −30 °C for several weeks to induce the deposition of green crystals of **4** (0.024 g, 7%).

Computational Details. All theoretical calculations were performed using Gaussian98.[38] All calculations utilized a DFT method using the three-parameter exchange functional of Becke[39] and the correlation

(37) Legzdins, P.; Rettig, S. J.; Ross, K. J.; Batchelor, R. J.; Einstein, F. W. B. *Organometallics* **1995**, *14*, 5579−5587.

(38) Frisch, M. J.; Trucks, G. W.; Schlegel, H. B.; Scuseria, G. E.; Robb, M. A.; Cheeseman, J. R.; Zakrzewski, V. G.; Montgomery, J. J. A.; Stratmann, R. E.; Burant, J. C.; Dapprich, S.; Millam, J. M.; Daniels, A. D.; Kudin, K. N.; Strain, M. C.; Farkas, O.; Tomasi, J.; Barone, V.; Cossi, M.; Cammi, R.; Mennucci, B.; Pomelli, C.; Adamo, C.; Clifford, S.; Ochterski, J.; Petersson, G. A.; Ayala, P. Y.; Cui, Q.; Morokuma, K.; Rega, N.; Salvador, P.; Dannenberg, J. J.; Malick, D. K.; Rabuck, A. D.; Raghavachari, K.; Foresman, J. B.; Cioslowski, J.; Ortiz, J. V.; Baboul, A. G.; Stefanov, B. B.; Liu, G.; Liashenko, A.; Piskorz, P.; Komaromi, I.; Gomperts, R.; Martin, R. L.; Fox, D. J.; Keith, T.; Al-Laham, M. A.; Peng, C. Y.; Nanayakkara, A.; Challacombe, M.; Gill, P. M. W.; Johnson, B.; Chen, W.; Wong, M. W.; Andres, J. L.; Gonzalez, C.; Head-Gordon, M.; Replogle, E. S.; Pople, J. A. *Gaussian 98*, revision A.11.4; Gaussian, Inc.: Pittsburgh, PA, 2002.

Table 3. X-ray Crystallographic Data for Complexes **2**, **3**, **4**, and $Fe(NO)_3Cl$

crystal data	**2**	**3**	**4**	$Fe(NO)_3Cl$
empirical formula	$C_3H_5N_4O_3F_6PFe$	$F_8Fe_2N_6O_8P_2$	$BF_4FeN_3O_3$	$ClFeN_3O_3$
crystal habit, color	block, dark	block, green	platelet, green	needle, brown
crystal size (mm)	0.30 × 0.20 × 0.10	0.25 × 0.25 × 0.05	0.18 × 0.10 × 0.05	0.40 × 0.10 × 0.05
crystal system	triclinic	orthorhombic	monoclinic	trigonal
space group	$P\bar{1}$	$Pna2_1$	$P2_1/n$	$P6_3mc$
volume (Å^3)	577.4(2)	1537.9(4)	706.21(12)	268.9(1)
a (Å)[a]	7.472(1)	22.810(3)	9.167(1)	7.1701(15)
b (Å)	7.539(1)	7.5762(12)	7.5255(6)	7.1701(15)
c (Å)	12.357(1)	8.8993(14)	10.327(1)	6.0403(12)
α (°)	73.44(1)	90	90	90
β (°)	89.41(1)	90	97.571(5)	90
γ (°)	61.11(1)	90	90	120
Z	2	4	4	2
formula weight (g/mol)	345.93	537.70	232.7	181.33
density (calculated) (Mg/m^3)	1.99	2.32	2.19	2.24
absorption coefficient (cm^{-1})	15.32	2.234	2.186	3.216
F_{000}	340	1040	448	176
radiation	MoKα, 0.71069 Å	MoKα, 0.71069 Å	MoKα, 0.71069 Å	MoKα, 0.71069 Å
data refinement	**2**	**3**	**4**	$Fe(NO)_3Cl$
final R indices[b]	$R_1 = 0.068$, $wR_2 = 0.202$	$R_1 = 0.049$, $wR_2 = 0.114$	$R_1 = 0.032$, $wR_2 = 0.080$	$R_1 = 0.024$, $wR_2 = 0.058$
goodness-of-fit on F[2c]	1.08	1.13	1.09	1.21
largest diff. peak and hole (e$^-$Å^{-3})	0.65 and −0.66	0.98 and −0.53	0.65 and −0.68	0.50 and −0.33

[a] Cell dimensions based on: **2**, 4724 reflections, 6.3° ≤ 2θ ≤ 56.1°; **3**, 4908 reflections, 5.7° < 2θ < 55.9°, **4**, 4263 reflections, 6.4° < 2θ < 55.6°, $Fe(NO)_3Cl$, 1854 reflections, 6.6° ≤ 2θ ≤ 55.4°. [b] Number of observed reflections: **2**, 7048 ($I_o > 2\sigma I_o$); **3**, 1853 ($I_o > 2\sigma I_o$); **4**, 6257 ($I_o > 2\sigma I_o$); $Fe(NO)_3Cl$, 2302 ($I_o > 2\sigma I_o$). $R = \sum(||F_o| - |F_c||)/\sum|F_o|$; $wR = [\sum w(|F_o|^2 - |F_c|^2)^2/\sum wF_o^4]^{1/2}$. w: **2**, $w = [\sigma^2(F_o^2) + (0.1181 \cdot P)^2 + 0.55 \cdot P]^{-1}$, where $P = (\mathrm{Max}(F_o^2, 0) + 2 \cdot F_c^2)/3$; **3**, $w = [\sigma^2(F_o^2) + (0.0371 \cdot P)^2 + 4.6106 \cdot P]^{-1}$, where $P = (\mathrm{Max}(F_o^2, 0) + 2 \cdot F_c^2)/3$; **4**, $w = [\sigma^2(F_o^2) + (0.0351 \cdot P)^2 + 0.6957 \cdot P]^{-1}$, where $P = (\mathrm{Max}(F_o^2, 0) + 2 \cdot F_c^2)/3$; $Fe(NO)_3Cl$, $w = [\sigma^2(F_o^2) + (0.0158 \cdot P)^2 + 0.6061 \cdot P]^{-1}$, where $P = (\mathrm{Max}(F_o^2, 0) + 2 \cdot F_c^2)/3$. [c] GOF = $[\sum(w(F_o^2 - F_c^2|)^2)/$ degrees of freedom$]^{1/2}$.

functional of Lee, Yang, and Parr (B3LYP).[40] The LANL2DZ basis set included both Dunning and Hay's D95 sets for B, N, O, and F,[41] and the nonrelativistic electron core potential (ECP) sets of Hay and Wadt for Fe.[42] The 6-311+G(2d,2p) basis set included the 6-311G basis for B, N, O, and F,[43] and the Wachters−Hay basis set for Fe,[44,45] including the scaling factors and diffuse functions of Raghavachari and Trucks,[46] along with two sets of polarization functions on all atoms.

Geometry optimizations were performed in C_1 symmetry, and frequency calculations on optimized geometries established the absence of any imaginary frequencies. Energies are reported as the sum of electronic and zero-point energies.

X-ray Crystallography. Data collection for each structure was performed on a Rigaku/ADSC CCD diffractometer using graphite-monochromated Mo Kα radiation at −100 ±1 °C.

Data for **2** were collected to a maximum 2θ value of 56.1° in 0.50° oscillations with 43 s exposures. The Twinsolve function in CrystalClear[47] was used to index the data since it could not be indexed otherwise. The crystal was found to be a four-component twin with the components being related as follows: Components 1 and 2 were related by a 180.00° rotation around [1, −1, 0]. Components 1 and 3 were related by a 121.05° rotation around [0, 0, −1]. Components 1 and 4 were related by a 180.00° rotation around [1, 0, 0]. Components 2 and 3 were related by a 180.00° rotation around [0, −1, 0]. Components 2 and 4 were related by a 121.11° rotation around [0, 0, 1]. Components 3 and 4 were related by a 180.00° rotation around [−1, 1, 1]. The data were integrated by measuring the data for all twin components, including overlapped reflections. The structure was solved by direct methods[48] using a HKLF 4 data set (containing only nonoverlapped reflections from component 1) and expanded using Fourier techniques.[49] Refinements were carried out using a HKLF 5 data set (containing all reflections). Non-hydrogen atoms were refined anisotropically, while hydrogen atoms were included in calculated positions. The final cycle of full matrix least-squares refinement was based on 8925 observed reflections and 170 variable parameters.

Data for **3** were collected to a maximum 2θ value of 55.9° in 0.50° oscillations with 35 s exposures. The solid-state molecular structure was solved by direct methods[50] and expanded using Fourier techniques.[49] The PF_6^- counterion was found to be disordered between two orientations in a 50:50 ratio. The final cycle of full-matrix least-squares refinement was based on 1853 observed reflections and 290 variable parameters.

Data for **4** were collected to a maximum 2θ value of 55.6° in 0.50° oscillations with 47 s exposures. The solid-state molecular structure was solved by direct methods[50] and expanded using Fourier techniques.[49] The final cycle of full-matrix least-squares refinement was based on 1556 observed reflections and 109 variable parameters.

Data for $Fe(NO)_3Cl$ were collected to a maximum 2θ value of 55.4° in 0.50° oscillations with 35 s exposures. The solid-state molecular structure was solved by direct methods[50] and expanded using Fourier techniques.[49] The final cycle of full-matrix least-squares refinement was based on 231 observed reflections and 19 variable parameters.

For each structure neutral atom scattering factors were taken from Cromer and Waber.[51] Anomalous dispersion effects were included in F_{calc};[52] the values for $\Delta f'$ and $\Delta f''$ were those of Creagh and McAuley.[53]

(39) Becke, A. D. *J. Chem. Phys.* **1993**, *98*, 5648−5652.
(40) Lee, C.; Yang, W.; Parr, R. G. *Phys. Rev.* **1988**, *B37*, 785−789.
(41) Dunning, T. H.; Hay, P. J. In *Modern Theoretical Chemistry*; Schaefer, H. F., III, Ed.; Plenum Press: New York, 1976; pp 1−28.
(42) Hay, P. J.; Wadt, W. R. *J. Chem. Phys.* **1985**, *82*, 299−310.
(43) Krishnan, R.; Binkley, J. S.; Seeger, R.; Pople, J. A. *J. Chem. Phys.* **1980**, *72*, 650−654.
(44) Hay, P. J. *J. Chem. Phys.* **1977**, *66*, 4377−4384.
(45) Wachters, A. J. H. *J. Chem. Phys.* **1970**, *52*, 1033−1036.
(46) Raghavachari, K.; Trucks, G. Q. *J. Chem. Phys.* **1989**, *91*, 1062−1065.
(47) CrystalClear: Version1.3.5b20; Molecular Structure Corporation, 2002.
(48) Altomare, A.; Burla, M. C.; Cammalli, G.; Cascarano, M.; Giacovazzo, C.; Guagliardi, A.; Moliterni, A. G. G.; Polidori, G.; Spagna, A. *J. Appl. Crystallogr.* **1999**, *32*, 115−119.
(49) DIRDIF94: Beurskens, P. T.; Admiraal, G.; Beurskens, G.; Bosman, W. P.; de Gelder, R.; Israel, R.; Smits, J. M. M. The DIRDIF-94 program system, Technical Report of the Crystallography Laboratory; University of Nijmegen, The Netherlands, 1994.
(50) Altomare, A.; Cascarano, M.; Giacovazzo, C.; Guagliardi, A. *J. Appl. Crystallogr.* **1993**, *26*, 343.
(51) Cromer, D. T.; Waber, J. T. *International Tables for X-ray Crystallography*; Kynoch Press: Birmingham, 1974; Vol. IV.
(52) Ibers, J. A.; Hamilton, W. C. *Acta Crystallogr.* **1964**, *17*, 781−782.
(53) Creagh, D. C.; McAuley, W. J. *International Tables for X-ray Crystallography*; Kluwer Academic Publishers: Boston, 1992; Vol. C.

The values for mass attenuation coefficients are those of Creagh and Hubbell.[54] All of the calculations were performed using the CrystalClear software package of Rigaku/MSC[47] or Shelxl-97.[55] X-ray crystallographic data for **2**, **3**, **4**, and $Fe(NO)_3Cl$ are collected in Table 3, and full details of all crystallographic analyses are provided in the Supporting Information.

Acknowledgment. We are grateful to the Natural Sciences and Engineering Research Council of Canada for support of this research in the form of grants to P.L. and postgraduate fellowships to T.W.H. P.L. is a Canada Council Killam Research Fellow.

(54) Creagh, D. C.; Hubbell, J. H. *International Tables for X-ray Crystallography*; Kluwer Academic Publishers: Boston, 1992; Vol. C.
(55) SHELXL97: Sheldrick, G. M. University of Göttingen, Germany, 1997.

Supporting Information Available: Details of the X-ray crystallographic studies and the DFT calculations (PDF and CIF). This material is available free of charge via the Internet at http://pubs.acs.org.

JA036887R